

MODELLING THE TEMPERATURE, MATURITY AND MOISTURE CONTENT IN A DRYING CONCRETE BLOCK

J. Charpin, T. Myers*, A. Sjöberg[†], Y. Ballim[‡]

Workshop participants: Jaco Bruyns, Jean Charpin, Corrie Lock, O Daniel Makinde, Peter Y Mhone, Gift Muchatibaya, Tim Myers, Nneoma Ogbonna, Astri Sjöberg and Samuel M Tshehla

Abstract

In this paper we continue work from a previous Study Group in developing a model for the maturation of concrete. The model requires equations describing the temperature, moisture content and maturity (or amount of cement that has reacted with the water). Non-dimensionalisation is used to simplify the model and provide simple analytical solutions which are valid for early time maturation. A numerical scheme is also developed and simulations carried out for maturation over one day and then two months. For the longer simulation we also investigate the effect of building the block in a single pour or two stages.

1 Introduction

When cement is mixed with water to form concrete an exothermic reaction occurs. The heat from the reaction leads to thermal expansion of the concrete. When the concrete cools down it will contract and induce a stress in the material. If the stress is sufficiently large it can lead to cracking which

*Department of Mathematics and Applied Mathematics, University of Cape Town, Rondebosch 7701, South Africa. *e-mail:* jcharpin@maths.uct.ac.za, myers@maths.uct.ac.za

[†]Department of Applied Mathematics, Auckland Park campus, University of Johannesburg, P.O. Box 524, Auckland Park, 2006, South Africa. *e-mail:* asjoberg@uj.ac.za

[‡]School of Civil and Environmental Engineering, University of the Witwatersrand, Wits 2050, Johannesburg, South Africa. *e-mail:* Yunnus.Ballim@wits.ac.za

obviously impairs the quality of the structure. With small concrete sections, surface cooling can quickly remove the heat and the resultant stresses will not be large. With large sections of concrete the temperature increase can be high, the surface cooling is slow and over long time periods very high stresses can build up. For this reason large concrete structures, such as dams, are built sequentially. New layers are only added when the earlier ones have cooled down and contracted sufficiently.

The build up of heat in a concrete block is caused by the concrete reacting with water. Therefore in order to model the temperature evolution in a concrete block it is necessary to describe the water content (the moisture) as well as the proportion of cement available to react with the water (this is measured in terms of *maturity*). Knowledge of these variables is important for other reasons as well. If the water is used up before all the cement has reacted the maturing process will end prematurely and the concrete does not reach its optimal strength. Pavlik *et al* [1] point out that the mould around a concrete block can only be removed after the concrete has reached a certain strength, which depends on the curing process. They go on to describe a microwave technique for measuring water content as a means of determining the concrete maturity. West & Holmes [2] investigate the problem of damage to impervious concrete floor coverings. This problem arises because builders often do not wait for the concrete to cure properly before finishing the floor. Further, current tests to determine when the floor can be finished only measure the concrete surface moisture content, neglecting the moisture further down in the block.

An understanding of the temperature, moisture content and maturity of concrete is therefore important in determining when to add new layers of concrete. It also helps determine the strength and possibility of cracking. At the first South African Mathematics in Industry Study Group 2004 the problem of modelling the maturing of a concrete block was introduced by the Cement & Concrete Institute. The initial model developed during the meeting and subsequently is described in [3]. The task of the Study Group was to investigate analytical and numerical solutions of the system of equations that model temperature, moisture content and maturity subject to suitable boundary and initial conditions. In answer, in the present report we take the preliminary work of [3] and attempt to refine it, as well as provide solutions for practical situations. The model equations of [3] as well as our own refinements are discussed in Section 2. In Section 3 we write the problem in non-dimensional form and identify small parameters. This permits some simplifications that are used in Section 4 to provide simple analytical solutions. In Section 5 we describe a numerical scheme to solve

the full system of equations. Results are presented for simulations over one day and two months. We also consider the effect of adding a second concrete layer after one month. The notation and typical values of the constants are given in the nomenclature in Section 7.

2 Model equations

In the original Study Group report [3] the following equations were derived:

$$\rho_c c_c \frac{\partial T}{\partial t} = \kappa \frac{\partial^2 T}{\partial x^2} + \gamma \frac{\partial m}{\partial t}, \quad (1)$$

$$\frac{\partial m}{\partial t} = \mu(1-m)\theta e^{-E/RT}, \quad (2)$$

$$\frac{\partial \theta}{\partial t} = \frac{\partial}{\partial x} \left(D(\theta) \frac{\partial \theta}{\partial x} \right) - \eta \frac{\partial m}{\partial t}, \quad (3)$$

where T , m and θ denote the temperature, maturity and moisture of the concrete respectively. All coefficients, with the exception of the diffusion, $D(\theta)$, are constant. In [3] it was suggested that the diffusion coefficient $D \sim e^{3\theta}$ but then θ was set to 1 throughout the slab and so D became constant. Equation (1) is the standard heat equation with a source term due to the chemical reaction. The maturity is a measure of the amount of cement that has reacted with the water. The maturity variation is governed by an Arrhenius type equation, namely equation (2). Finally, the water content or moisture must also satisfy a diffusion equation. The sink term, $-\eta m_t$ in equation (3), indicates that water is used up in the reaction. The notation is defined in the nomenclature, Section 7.

The initial and boundary conditions used in [3] were

$$m(x, 0) = 0 \quad \theta(x, 0) = \theta_i \quad T(x, 0) = T_i .$$

At the free surface the temperature was prescribed

$$T(L, t) = T_1 + T_d \sin \omega_d t + T_m \sin \omega_m t, \quad (4)$$

which reflects the daily and monthly temperature variation. Evaporation was accounted for by

$$-D_m \left. \frac{\partial \theta(x, t)}{\partial x} \right|_{x=L} = \bar{e}(\theta_a - \theta(L, t)). \quad (5)$$

Finally, symmetry was imposed at the centre of the block

$$\frac{\partial \theta}{\partial x} = \frac{\partial T}{\partial x} = 0 .$$

As the basis of our work we will use the above equations (1 – 3). However, it should be noted that these equations were part of a preliminary study and as such involved certain simplifications that may be improved upon in this follow-on study. The modifications are as follows:

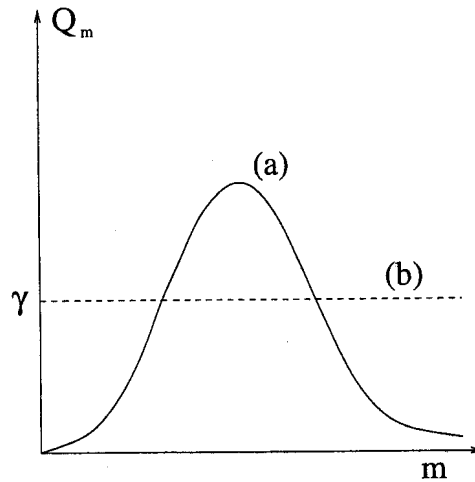


Figure 1: Variation of Q_m with m and a constant approximation.

1. The final term of equation (1), namely γm_t where γ is constant, should read Q_t , since it represents the heat generation. It may be expressed in terms of the maturity by $Q_t = Q_m m_t$, hence in the previous work $\gamma \sim Q_m$. A typical form for Q_m is shown by curve (a) in Figure 1, where the dotted line (b) represents the constant approximation. Clearly curve (a) is far from constant and so we will replace the constant value for γ with a curve of the form

$$\gamma = Q_m = A m e^{-a m^2} . \quad (6)$$

If the maximum value of Q_m occurs at (m_x, Q_x) then $a = 1/2m_x^2$ and $A = Q_x \sqrt{e}/m_x$.

2. The surface temperature boundary condition, equation (4), basically states that the temperature is known (and matches the ambient temperature). This is a reasonable first approximation, however, in general a cooling condition will provide a more accurate model. This was investigated in [4] for exactly this problem. In that report it was shown that the concrete surface temperature lags behind the air temperature and is also greatly affected by the sun. This result agrees with experimental measurements. A more reasonable boundary condition is therefore

$$-\kappa \frac{\partial T}{\partial x} = Q_s + H(T - T_a) , \quad (7)$$

where Q_s represents the solar radiation and T_a the ambient temperature. Both can be functions of time and, in particular, if we let T_a be defined by the right hand side of equation (4) then we correctly include the ambient temperature variation. Equation (4) is valid over long time periods. Since our interest is in shorter time-scales, in the numerical solutions of Section 5 we will neglect the monthly variation.

3. The bottom of any block, which is placed on the ground or another block, will be subject to very different conditions to the top, which is exposed to the air. Hence symmetry is not appropriate. Instead we assume the bottom is insulated. This could represent a block on soil or some other relatively poor conductor. However, the block could be on top of rock which is a good conductor, and so a different condition will be required. In the absence of information we choose the insulated condition.
4. The diffusion coefficient in equation (3) may vary with moisture. The variation is discussed by West *et al* [2]. Their results show a maximum variation in the range $[1, 5] \times 10^{-9} \text{m}^2/\text{s}$ (provided you interpret their unsound axes correctly). They also provide a closed form algebraic expression for the variation. A simpler representation is given by

$$D(\theta) = D_m [\alpha + (1 - \alpha)(1 + \tanh a(\theta - \theta_m))] \quad (8)$$

where $D_m \sim 2 \times 10^{-9} \text{m}^2/\text{s}$, $\alpha \sim 0.05$, $\theta_m \sim 0.8$ and $a \sim 20$. We will take D as constant $D \sim 2 \times 10^{-9} \text{m}^2/\text{s}$ when calculating analytical results. In the numerical results we will allow for diffusion variation.

The boundary condition (5) is modified to

$$-D(\theta(L, t)) \left. \frac{\partial \theta(x, t)}{\partial x} \right|_{x=L} = \bar{e}(\theta_a - \theta(L, t)) . \quad (9)$$

West *et al* [2] also discuss the evaporation rate \bar{e} which occurs in equation (5). This rate actually decreases slowly with time. However, the decrease, in a controlled room, is around 5% after 50 days. In the laboratory the decrease is around 17% after 90 days, hence we will take it as constant, $\bar{e} \sim 1.8 \times 10^{-9}$ m/s.

With the model set up, we now proceed to non-dimensionalise the equations.

3 Non-dimensional equations

The variables are now non-dimensionalised in the following manner

$$\hat{x} = \frac{x}{L} \quad \hat{t} = \frac{t}{\tau} \quad \hat{T} = \frac{T - T_i}{\bar{T}_a - T_i} = \frac{T - T_i}{\Delta T} \quad \hat{\theta} = \frac{\theta}{\theta_i} \quad \hat{D} = \frac{D}{D_m}$$

$$\hat{Q}_m = \frac{Q_m}{A},$$

where \bar{T}_a is the average ambient temperature and τ is the time-scale. The maturity is a fraction between 0 and 1 and is already non-dimensional. We immediately drop the hat notation.

The non-dimensional equations governing the problem are:

$$\frac{\partial T}{\partial t} = \alpha_1 \frac{\partial}{\partial x} \left(\frac{\partial T}{\partial x} \right) + \alpha_2 Q_m \frac{\partial m}{\partial t}, \quad (10)$$

$$\frac{\partial m}{\partial t} = \alpha_3 (1 - m) \theta e^{1/(\alpha_4 + \alpha_5 T)}, \quad (11)$$

$$\frac{\partial \theta}{\partial t} = \alpha_6 \frac{\partial}{\partial x} \left(D(\theta) \frac{\partial \theta}{\partial x} \right) - \alpha_7 \frac{\partial m}{\partial t}, \quad (12)$$

where the constants $\alpha_1, \dots, \alpha_7$ are defined by:

$$\alpha_1 = \frac{\kappa \tau}{\rho_c c_c L^2}, \quad \alpha_2 = \frac{Q_x \sqrt{e}}{\rho_c c_c \Delta T m_x}$$

$$\alpha_3 = \tau \mu \theta_i, \quad \alpha_4 = -\frac{RT_i}{E}, \quad \alpha_5 = -\frac{R \Delta T}{E}$$

$$\alpha_6 = \frac{\tau D_m}{L^2}, \quad \alpha_7 = \frac{\eta}{\theta_i},$$

and

$$Q_m = m e^{-m^2/(2m_x^2)}. \quad (13)$$

The corresponding boundary conditions are:

α_1	7.36×10^{-5}	α_2	21.26	α_3	1000
α_4	-0.07	α_5	-6×10^{-3}	α_6	2×10^{-7}
α_7	1.25	β_2	-10.94	β_3	-2.7

Table 1: Values for α_i, β_i with $i = 1, 2, \dots, 7$.

- At $t = 0$, temperature, maturity and moisture are constant throughout the layer

$$T(x, 0) = 0, \quad m(x, 0) = 0, \quad \theta(x, 0) = 1. \quad (14)$$

- At $x = 0$, the block is insulated for temperature and moisture:

$$\left. \frac{\partial T}{\partial x} \right|_{x=0} = 0, \quad \left. \frac{\partial \theta}{\partial x} \right|_{x=0} = 0. \quad (15)$$

- At $x = 1$, a flux condition is imposed for temperature and moisture:

$$\left. \frac{\partial T}{\partial x} \right|_{x=1} = \beta_1 + \beta_2 T|_{x=1}, \quad \left(D(\theta) \frac{\partial \theta}{\partial x} \right) \Big|_{x=1} = -\beta_3 (\theta|_{x=1} - \theta_a), \quad (16)$$

where the constants β_1, β_2 and β_3 are defined by:

$$\beta_1 = -\frac{Q_s L + HL(T_i - T_a)}{\kappa \Delta T}, \quad \beta_2 = -\frac{HL}{\kappa}, \quad \beta_3 = \frac{L\bar{e}}{D_m}. \quad (17)$$

Typical values for α_i and β_i are given in Table 1. If the ambient temperature is taken as constant (for example if we are interested in solutions over a short period) then $T_a = 1$, otherwise $\beta_1 = \beta_1(t)$. Typical values for other parameters are given with the definitions in the nomenclature section.

4 Model simplifications

Consider the parameter values shown in Table 1. The diffusion parameters α_1 and α_6 are both small. Physically this means that diffusion is, in general, slow and consequently the x variation of T and θ is negligible throughout most of the domain. Neglecting the x derivatives means we are unable to satisfy the boundary conditions. Since we choose $T_x = \theta_x = 0$ at the bottom an x independent solution is automatically satisfied there. However,

to satisfy the upper conditions, a boundary layer must be present in the vicinity of $x = 1$.

A standard boundary layer scaling indicates the appropriate layer thicknesses are given by $L_T = \sqrt{\alpha_1}$ and $L_m = \sqrt{\alpha_6}$ respectively. Using the values given in Table 1 we expect $L_T \approx 1\text{cm}$, $L_m \approx 0.5\text{mm}$. In our subsequent numerical solutions a boundary layer of around 2cm may be observed on some of the maturity curves (see the 35, 40 and 60 day curves on Figure 10 for example). However, in general, the fluctuations in the ambient temperature prevents us from seeing the boundary layer. We also see no benefit in carrying out the boundary layer analysis since when we rescale in the boundary layers we end up retaining all terms in the governing equations, even the original boundary conditions hold. Hence we may as well solve the original system in the first place. Instead we will now simply look at the solution in the bulk.

Neglecting the small diffusion terms in equations (10) and (12), our temperature and moisture equations are

$$\frac{\partial T}{\partial t} = \alpha_2 Q_m \frac{\partial m}{\partial t}, \quad \frac{\partial \theta}{\partial t} = -\alpha_7 \frac{\partial m}{\partial t}. \quad (18)$$

The second equation in (18) integrates immediately to determine the moisture in terms of the maturity

$$\theta = 1 - \alpha_7 m, \quad (19)$$

so the moisture decreases linearly with maturity.

With the definition of Q_m given by equation (13) we find

$$T = \alpha_2 m_x^2 \left(1 - e^{-m^2/(2m_x^2)} \right). \quad (20)$$

We could now replace T and θ in the maturity equation (11), resulting in a first order differential equation to solve numerically, and hence determine the bulk solution for m . An alternative approach is to note that the exponential term in the maturity equation (11) contains $\alpha_4 + \alpha_5 T$. Since $\alpha_4 \sim 10\alpha_5$ we may neglect the term $\alpha_5 T$, provided T remains small. Hence a reasonable approximation is to model maturity with

$$\frac{\partial m}{\partial t} = \alpha_3(1 - m)\theta e^{1/\alpha_4}. \quad (21)$$

Substituting for θ from equation (19) into equation (21) leads to a first order separable equation for m ,

$$\frac{\partial m}{\partial t} = \alpha_3(1 - m)(1 - \alpha_7 m)e^{1/\alpha_4}. \quad (22)$$

The solution is

$$m = \frac{1 - e^{(\alpha_3 e^{1/\alpha_4})(\alpha_7 - 1)t}}{1 - \alpha_7 e^{(\alpha_3 e^{1/\alpha_4})(\alpha_7 - 1)t}}. \quad (23)$$

If $\alpha_7 = 1$ we find the limiting case

$$m = \frac{(\alpha_3 e^{1/\alpha_4}) t}{1 + (\alpha_3 e^{1/\alpha_4}) t}. \quad (24)$$

The corresponding solutions for the moisture θ are:

$$\theta = 1 - \alpha_7 \frac{1 - e^{(\alpha_3 e^{1/\alpha_4})(\alpha_7 - 1)t}}{1 - \alpha_7 e^{(\alpha_3 e^{1/\alpha_4})(\alpha_7 - 1)t}} \quad (25)$$

and in the limiting case when $\alpha_7 = 1$

$$\theta = 1 - \frac{(\alpha_3 e^{1/\alpha_4}) t}{1 + (\alpha_3 e^{1/\alpha_4}) t}. \quad (26)$$

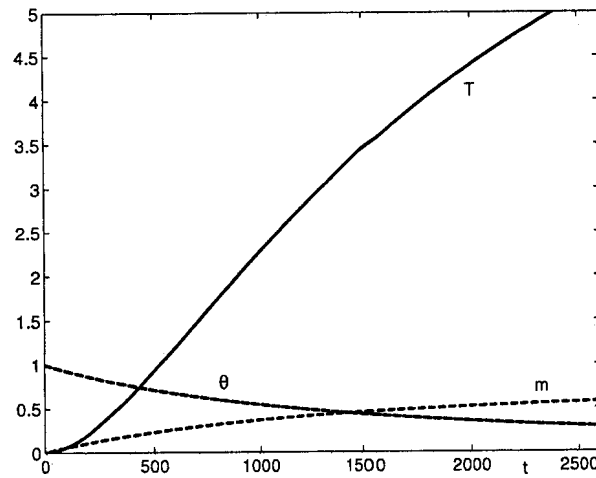


Figure 2: Variation of m , θ and T with time t .

The variation of m , θ and T are shown in Figure 2. The time-scale $\tau = 1000$ s and the temperature scale $\Delta T = 25$ K, so this simulation which runs to $t \approx 2600$ corresponds to 30 days. The maturity increases monotonically,

tending to the asymptote $1/\alpha_7 = 0.8$. After 30 days it is still well below this value at $m \sim 0.57$. The moisture θ decreases as m increases. The temperature also increases towards an asymptote but is not close to the asymptote after 30 days. The temperature rise is rather high. With the scale of 25K we see that the rise is around 125K over 30 days. This can be attributed to the neglect of the cooling condition at the free surface. There is no mechanism for heat to escape and consequently it builds up very rapidly. This has consequences in the neglecting of the term $\alpha_5 T$ in the maturity equation. Since T builds up rapidly this approximation can only hold for short time periods, of the order of days. We show this in subsequent graphs in the numerical section. In particular, in Figure 7, we show that the maturity approximation is excellent after 2 days with only a small difference at the free surface. After 10 days there is a 15% difference between analytical and numerical bulk solutions.

In general, of the three curves we expect the temperature to be the least realistic. The maturity satisfies a first order ordinary differential equation, and we satisfy the initial condition. The temperature and moisture both satisfy diffusion equations, however, we neglect the diffusion terms. In both cases we satisfy the initial condition and the boundary condition at $x = 0$, but cannot satisfy the surface condition. However, the coefficient $\alpha_6 \ll \alpha_1$ and so we expect the largest boundary layer effect with the temperature equation. Hence we expect m to give the best approximation, then θ and finally T is probably the worst. We will investigate this further when we solve the full equations numerically.

From these results we can make a statement about α_7 . Firstly, if $\alpha_7 > 1$ then as $t \rightarrow \infty$ the exponential terms dominate in equation (23) and $m \rightarrow 1/\alpha_7$. Hence the maturity can never reach unity. If $\alpha_7 < 1$ then as $t \rightarrow \infty$ the exponential terms decay and the maturity $m \rightarrow 1$. If $\alpha_7 = 1$ we also find $m \rightarrow 1$. Experimental results show that the maturity typically increases to a maximum of around $m = 0.8$. This motivates our choice $\alpha_7 = 1.25$. Practically by taking a number of maturity measurements over time, we could estimate all the parameters α_3, α_4 and α_7 in the maturity equation.

5 Numerical method and solutions

5.1 Numerical scheme

The system will now be solved numerically, using a standard finite difference method. The three parameters T , m and θ are calculated on equally spaced points numbered from 0 to n_x , including the boundaries, separated by the

space step $\Delta x = 1/n_x$. The simulation time t_m is divided in n_t time steps denoted $\Delta t = t_m/n_t$. The temperature, maturity and moisture at $x = i\Delta x$ and $t = k\Delta t$ are denoted T_i^k , m_i^k , θ_i^k respectively.

To slightly simplify the system, the equations may be rewritten:

$$\frac{\partial T}{\partial t} = \alpha_1 \frac{\partial^2 T}{\partial x^2} + \alpha_2 \alpha_3 Q_m(m)(1-m)\theta e^{1/(\alpha_4 + \alpha_5 T)}, \quad (27)$$

$$\frac{\partial m}{\partial t} = \alpha_3(1-m)\theta e^{1/(\alpha_4 + \alpha_5 T)}, \quad (28)$$

$$\frac{\partial \theta}{\partial t} = \alpha_6 \frac{\partial}{\partial x} \left(D(\theta) \frac{\partial \theta}{\partial x} \right) - \alpha_3 \alpha_7 (1-m)\theta e^{1/(\alpha_4 + \alpha_5 T)}. \quad (29)$$

Equations (27) and (29) are diffusion equations with respectively a source and a sink term. They involve second order space derivatives that are key in the stability of the numerical scheme. They will be discretised with a partially implicit scheme:

- The space derivatives are discretised using an implicit method to guarantee good stability of the numerical scheme,
- The two parameters, $D(\theta)$ and $Q_m(m)$, and the source and sink terms are discretised with an explicit method. In theory, they could also be discretised with an implicit method but the resolution of the system would become too time consuming.

Equation (28) does not involve any space derivative and may be discretised using an explicit method.

Using the standard finite volume method leads to the following difference equations:

- Temperature

In general we use

$$-\left[\frac{2\alpha_1 \Delta t}{\Delta x^2} \right] T_{i+1}^{k+1} + \left[1 + \frac{2\alpha_1 \Delta t}{\Delta x^2} \right] T_i^{k+1} - \left[\frac{2\alpha_1 \Delta t}{\Delta x^2} \right] T_{i-1}^{k+1} = T_i^k + \alpha_2 \alpha_3 \Gamma_i \Delta t. \quad (30)$$

At the boundary $x = 0$ we apply $T_x = 0$ from equation (15) and so impose

$$\left[1 + \frac{2\alpha_1 \Delta t}{\Delta x^2} \right] T_0^{k+1} - \left[\frac{2\alpha_1 \Delta t}{\Delta x^2} \right] T_1^{k+1} = T_0^k + \alpha_2 \alpha_3 \Gamma_0 \Delta t. \quad (31)$$

At $x = 1$ we apply equation (16) and set

$$-\left[\frac{2\alpha_1\Delta t}{\Delta x^2}\right]T_{n_x-1}^{k+1} + \left[1 + \frac{2\alpha_1\Delta t}{\Delta x^2} - \frac{2\alpha_1\beta_2\Delta t}{\Delta x}\right]T_{n_x-1}^{k+1} = T_{n_x}^k + \frac{2\alpha_1\beta_1\Delta t}{\Delta x} + \alpha_2\alpha_3\Gamma_n\Delta t, \quad (32)$$

where

$$\begin{aligned} \Gamma_0 &= \frac{\Delta x}{4} \left[(1 - m_0)Q_m(m_0)\theta_0 e^{1/(\alpha_4 + \alpha_5 T_0)} \right. \\ &\quad \left. + (1 - m_{1/2})Q_m(m_{1/2})\theta_{1/2} e^{1/(\alpha_4 + \alpha_5 T_{1/2})} \right], \\ \Gamma_i &= \frac{\Delta x}{2} \left[(1 - m_{i-1/2})Q_m(m_{i-1/2})\theta_{i-1/2} e^{1/(\alpha_4 + \alpha_5 T_{i-1/2})} \right. \\ &\quad \left. + (1 - m_{i+1/2})Q_m(m_{i+1/2})\theta_{i+1/2} e^{1/(\alpha_4 + \alpha_5 T_{i+1/2})} \right], \\ &\quad 1 \leq i \leq n_x - 1, \\ \Gamma_{n_x} &= \frac{\Delta x}{4} \left[(1 - m_{n_x-1/2})Q_m(m_{n_x-1/2})\theta_{n_x-1/2} e^{1/(\alpha_4 + \alpha_5 T_{n_x-1/2})} \right. \\ &\quad \left. + (1 - m_{n_x})Q_m(m_{n_x})\theta_{n_x} e^{1/(\alpha_4 + \alpha_5 T_{n_x})} \right], \\ T_{i+1/2} &= \frac{T_i + T_{i+1}}{2}, \quad m_{i+1/2} = \frac{m_i + m_{i+1}}{2}, \quad \theta_{i+1/2} = \frac{\theta_i + \theta_{i+1}}{2}. \end{aligned}$$

- Maturity

$$m_i^{k+1} = m_i^k + \Delta t \alpha_3 (1 - m_i^k) \theta_i^k e^{1/(\alpha_4 + \alpha_5 T_i^k)} \quad 0 \leq i \leq n_x. \quad (33)$$

- Moisture

In general we apply

$$\begin{aligned} &-\left[\frac{2\alpha_6\Delta t}{\Delta x^2}D\left(\theta_{i+1/2}^k\right)\right]\theta_{i+1}^{k+1} \\ &+ \left[1 + \frac{2\alpha_6\Delta t}{\Delta x^2}\left(D\left(\theta_{i+1/2}^k\right) + D\left(\theta_{i-1/2}^k\right)\right)\right]\theta_i^{k+1} \\ &- \left[\frac{2\alpha_6\Delta t}{\Delta x^2}D\left(\theta_{i-1/2}^k\right)\right]\theta_{i-1}^{k+1} = \theta_i^k + \alpha_3\alpha_7\Lambda_i\Delta t. \quad (34) \end{aligned}$$

At $x = 0$ we apply $\theta_x = 0$ from equation (15) and so impose

$$\begin{aligned} & \left[1 + \frac{2\alpha_6\Delta t}{\Delta x^2} D(\theta_{1/2}^k) \right] \theta_0^{k+1} \\ & - \left[\frac{2\alpha_6\Delta t}{\Delta x^2} D(\theta_{3/2}^k) \right] \theta_1^{k+1} = \theta_0^k + \alpha_3\alpha_7\Lambda_0\Delta t. \end{aligned} \quad (35)$$

At $x = 1$ we apply equation (16) and set

$$\begin{aligned} & - \left[\frac{2\alpha_6\Delta t}{\Delta x^2} D(\theta_{n_x-1/2}^k) \right] \theta_{n_x-1}^{k+1} \\ & + \left[1 + \frac{2\alpha_6\Delta t}{\Delta x^2} D(\theta_{n_x-1/2}^k) - \frac{2\alpha_6\beta_3\Delta t}{\Delta x} \right] \theta_{n_x-1}^{k+1} \\ & = \theta_{n_x}^k + \frac{2\alpha_6\beta_3\theta_a\Delta t}{\Delta x} D(\theta_{n_x}^k) + \alpha_3\alpha_7\Lambda_n\Delta t, \end{aligned} \quad (36)$$

where

$$\begin{aligned} \Lambda_0 &= \frac{\Delta x}{4} \left[(1 - m_0)\theta_0 e^{1/(\alpha_4 + \alpha_5 T_0)} + (1 - m_{1/2})\theta_{1/2} e^{1/(\alpha_4 + \alpha_5 T_{1/2})} \right], \\ \Lambda_i &= \frac{\Delta x}{2} \left[(1 - m_{i-1/2})\theta_{i-1/2} e^{1/(\alpha_4 + \alpha_5 T_{i-1/2})} \right. \\ & \quad \left. + (1 - m_{i+1/2})\theta_{i+1/2} e^{1/(\alpha_4 + \alpha_5 T_{i+1/2})} \right], \quad 1 \leq i \leq n_x - 1, \\ \Lambda_{n_x} &= \frac{\Delta x}{4} \left[(1 - m_{n_x-1/2})\theta_{n_x-1/2} e^{1/(\alpha_4 + \alpha_5 T_{n_x-1/2})} \right. \\ & \quad \left. + (1 - m_{n_x})\theta_{n_x} e^{1/(\alpha_4 + \alpha_5 T_{n_x})} \right]. \end{aligned}$$

Equation (33) leads directly to the maturity at time $t = (k + 1)\Delta t$. Equations (31–32) and (35–36) form two tri-diagonal systems of n_x linear equations each of n_x unknowns, namely the values of T and θ at time $t = (k + 1)\Delta t$. These two systems may be solved easily with an LU factorisation for example.

The numerical scheme is now complete so we move on to presenting the results.

5.2 Numerical solutions

The solutions of the governing equations will be described in three different situations. Firstly the evolution of the variables will be studied during a single day, to evaluate the influence of the varying ambient conditions. Secondly, a two month simulation will be carried out, where the concrete

layer is built in a single stage. Finally, another two month simulation will be studied where the block is built in two stages, with the second stage being added after one month. The values of the constants used for all these simulations may be found in Table 1.

Temperature variation and sun exposure is represented as follows:

- Sunrise and sunset occur every day at 06:30 and 19:30 respectively.
- The minimum temperature $T_{min} = 288K$ occurs one hour before sunrise.
- The maximum temperature is $T_{max} = 303K$.
- Temperature variation during the day is modelled with a cosine function.

Using the definition given in Equation (17), the parameter β_1 may then be expressed as:

$$\beta_1 = 43.8f(t) - 3.28 \cos \left[\frac{2\pi}{24}(t - 5.5) \right],$$

where t represents the time of the day in hours and the function $f(t)$ defines the daylight hours, when solar radiation plays a role,

$$f(t) = \begin{cases} 1 & \text{if } 6.5 \leq t \leq 19.5, \\ 0 & \text{otherwise.} \end{cases}$$

In the three cases studied here, the simulation starts at midday (12:00).

5.2.1 One day simulation

Figure 3 shows the evolution of the temperature inside the concrete layer during the first 24 hours. Only the top of the layer is shown on the picture, for the heights $0.6 \leq x \leq 1$. The temperature does not vary in space for $x \leq 0.6$, so this part was excluded to make the picture clearer.

The initial temperature of the layer is $T = 0$. Temperature profiles corresponding to times $t = 15.00, 19.00, 20.00, 0.00(+1), 6.00(+1), 7.00(+1), 12.00(+1)$ are shown in Figure 3. Two heating effects can be observed. The chemical reaction leads to a slow release of energy which acts to increase the temperature throughout the block. We can see at $x = 0.6$ that there is a very small rise in the temperature. The boundary condition $T_x = 0$, imposed at $x = 0$, prevents energy from leaving at that boundary. Hence,

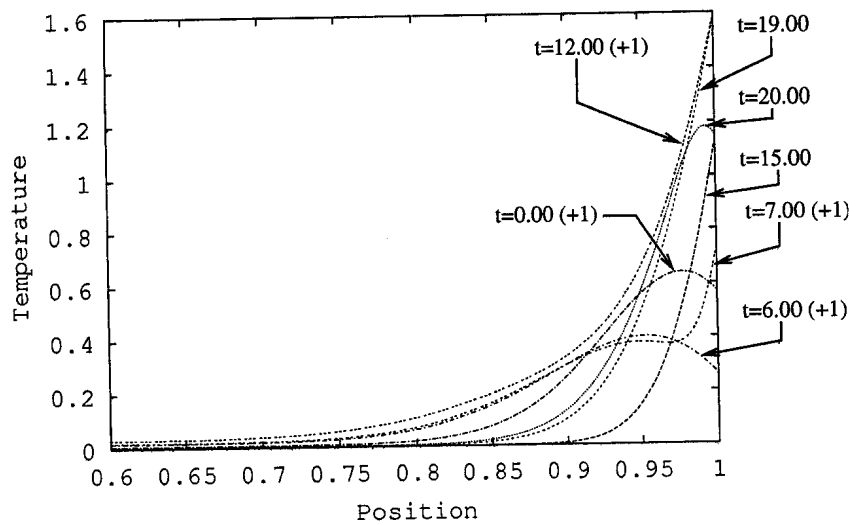


Figure 3: Evolution of the temperature profile during the first 24 hours

even though the hydration reaction is slow, the temperature must slowly increase inside the block.

In the vicinity of $x = 1$ we see the effect of the ambient temperature on the block. During day time, between 06:30 and 19:30 in the present case, the radiation of the sun heats the top of the layer very significantly. This causes the sudden increase of temperature at the surface. This effect is balanced by the influence of the ambient temperature. During the day, the ambient temperature is assumed to vary between $T_{min} = 15^{\circ}C$ and $T_{max} = 30^{\circ}C$ in dimensional form, corresponding to $T_{min} = -0.3$ and $T_{max} = 0.3$ in non-dimensional form. The surface temperature is well above $T = 0.3$ from the first hour so the ambient temperature cools the surface down. This effect is hard to notice during day time, but as soon as solar radiation stops, the temperature at $x = 1$ drops significantly. After 30 minutes without sun, at 20:00, the non-dimensional drop in temperature reaches $\Delta T = 0.4$. Just before sunrise, at 06:00, the surface temperature has dropped to $T = 0.3$ from $T \approx 1.6$ the previous day at 19:00. When the sun rises again, the temperature makes a significant jump and at the end of the first 24 hours, it has reached $T = 1.6$, slightly above the maximum temperature observed the previous day.

The heat gained at the surface slowly diffuses through the concrete layer. The variations at the surface of the layer only affect the temperature above

$x = 0.9$ at first. Progressively, the effects may be seen up to $x = 0.75$ after one day. However, during the first day, most of the heat inside the layer is released by the chemical reaction and heat diffusion is mainly observed at the top of the layer.

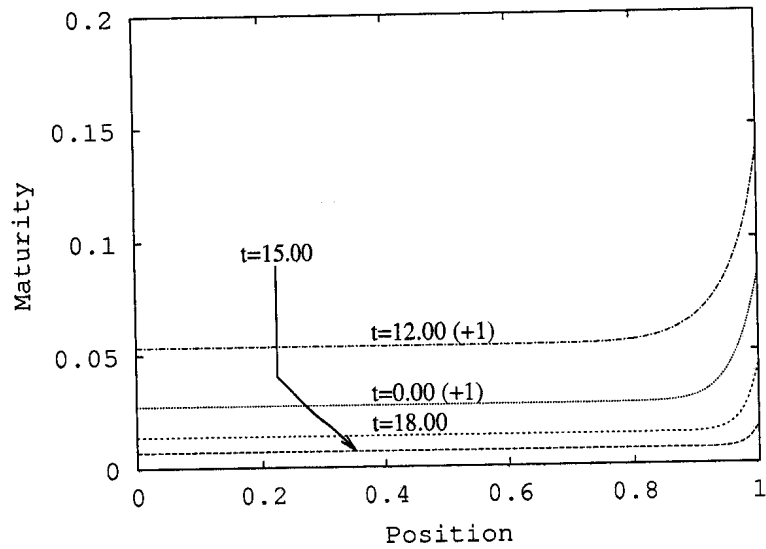


Figure 4: Evolution of the maturity profile during the first 24 hours

The evolution of the maturity over the first 24 hours is shown in Figure 4. The maturity increases slowly over the first few hours. After a day, just over 5% of the concrete hydration has happened. The reaction releases heat, causing the temperature rise observed in Figure 3. The maturity is approximately constant throughout the layer except near $x = 1$ where it is accelerated by the increase in surface temperature. Figure 5 shows the moisture variation. As the analytical solution suggests, the moisture variation is a mirror image of the maturity, $\theta = 1 - \alpha_7 m$. The moisture level after a day is just about 95% of the initial value. Since the water is used in the hydration process it is nearly constant throughout the layer and only decreases at the top of the layer where the reaction is more advanced. Neither diffusion nor the boundary conditions have a significant effect, the evolution is primarily due to the chemical reaction.

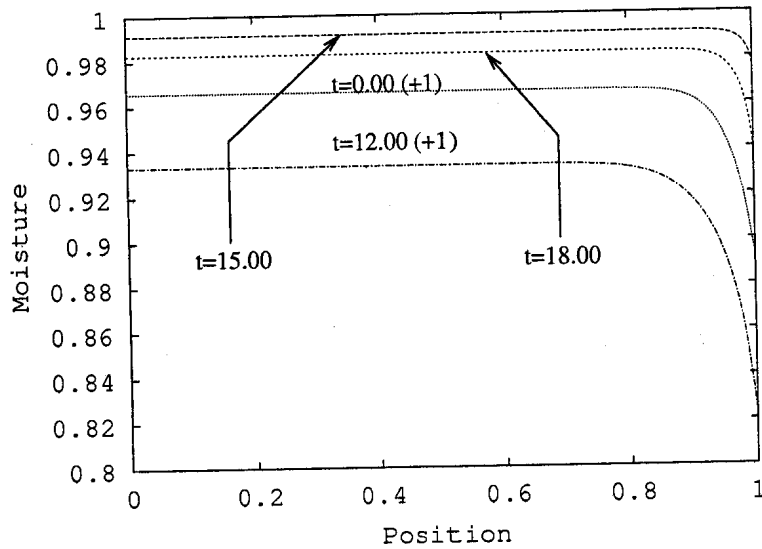


Figure 5: Evolution of the moisture profile during the first 24 hours

5.2.2 Two month simulation

The evolution is now studied on a much longer term. The daily variations are still taken into account in the simulation but for comparison purposes, the variables are always plotted at midday in the following two sections.

The variation of the maturity over the first two months may be seen in Figure 6. The trend observed in Figure 4 that the maturity is approximately constant through the bulk can still be seen, but as t increases the increase near $x = 1$ diffuses through the layer. After 60 days the maturity shows a very slight linear increase from $x = 0$ to around $x = 0.98$, followed by a small decrease. The maturity is everywhere slightly below its maximum possible value of 0.8. In Figure 7 we compare the numerical and analytical solutions for maturity after 2 and 10 days. After 2 days, the constant analytical solution and the numerical solution are nearly equal over most of the layer, they only differ near $x = 1$ where the external energy has accelerated the reaction in the numerical solution. After 10 days, a lot of heat has been released in the layer due to the hydration reaction. The numerical solution also feels the external energy input and this extra energy has diffused through the block. The result is that the analytical solution differs from the numerical one by about 15% in the bulk and the correspondence deteriorates as the top is

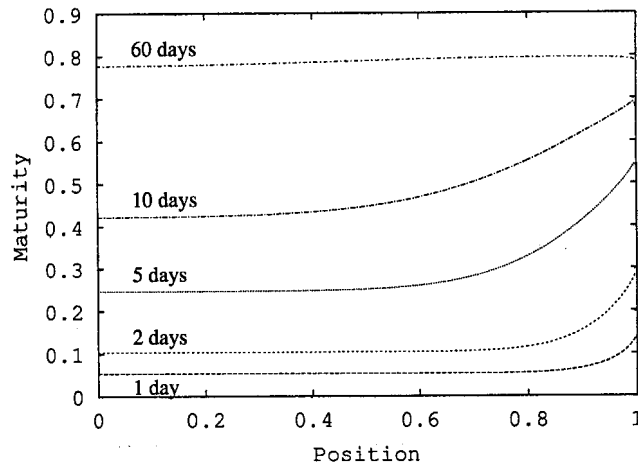


Figure 6: Evolution of the maturity profile during the first 2 months

approached. This result is in agreement with our earlier statement that the analytical solution will only hold for early times. The moisture evolution is

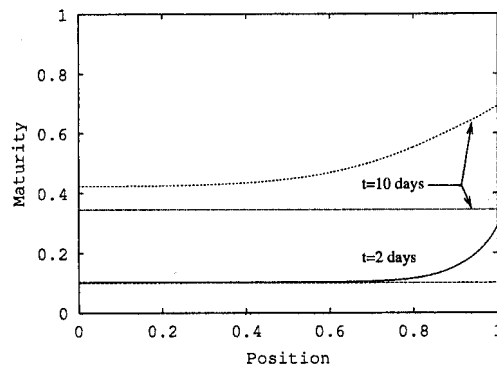


Figure 7: Comparison of numerical and analytical maturity curves

shown in Figure 8. The moisture slowly decreases throughout the block, but the decrease is most rapid near $x = 1$ where water is lost to the hydration reaction and evaporation. After 60 days we can see that for $x < 0.8$ there is a small amount of water remaining and so the hydration can continue for some time longer. For $x > 0.8$ the water has been used up and the

reaction can therefore only continue if water can diffuse in. Since diffusion is very slow this will slow the reaction down significantly. Hence, after 60 days both the maturity and moisture have almost reached their final limits. The temperature evolution, shown in Figure 9, behaves in a very different

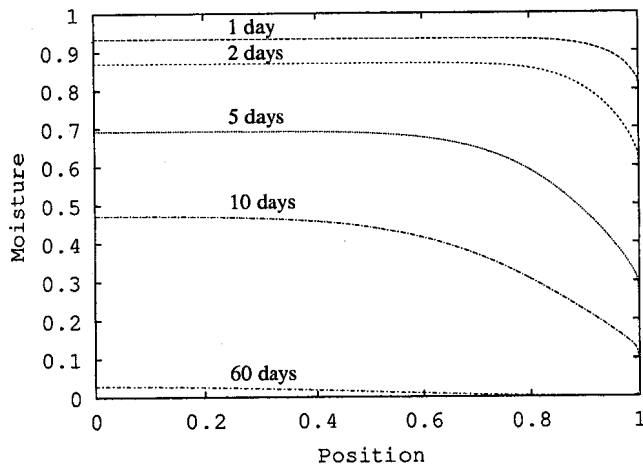


Figure 8: Evolution of the moisture profile during the first 2 months

manner. Temperature increase is due to the hydration reaction and energy gains or loss (at night) at the surface $x = 1$. The insulation condition at $x = 0$ prevents any heat loss there. Heat diffusion in concrete is very slow. The diffusion coefficient $D_c = \kappa/\rho_c c_c \sim 10^{-6} \text{m}^2/\text{s}$. Consequently we see a slow temperature rise near $x = 0$. Near $x = 1$ the temperature remains high at the boundary and this can be seen to diffuse through the layer. As t increases diffusion allows much of this energy to be spread through the layer, which will tend towards the average daily temperature. There will always be a boundary layer near $x = 1$ that reflects the daily variation, which does not have time to diffuse far.

5.2.3 Two month simulation with two layers

Finally, we investigate the effect of adding a second layer to the first after 30 days. We begin by running the simulation for a single block for 30 days. We then place an identical block on top, with the same initial conditions as the original block.

The maturity evolution is shown in Figure 10. A close up of the interface

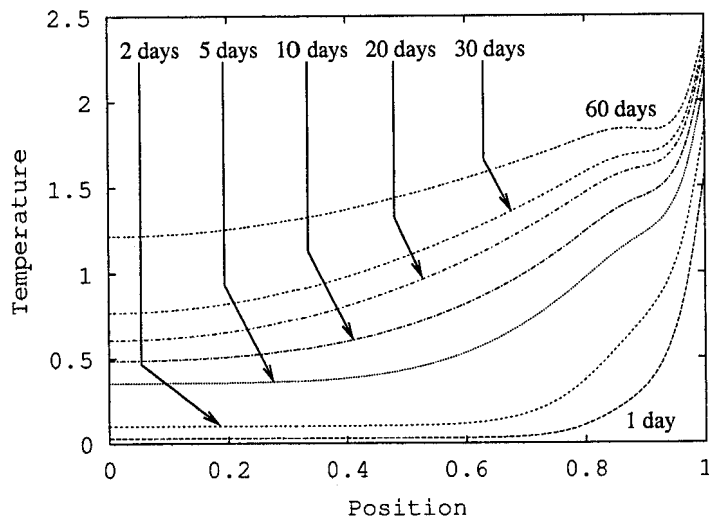


Figure 9: Evolution of the temperature profile during the first 2 months

is shown in Figure 11. The initial block has a maturity increasing from 0.68 to approximately 0.78 near $x = 1$ after 30 days. At this stage the reaction could be expected to proceed very slowly, particularly near $x = 1$ where the maturity is close to the maximum, $m = 0.8$. The addition of the second layer provides a new source of water for the top of the first block. This water diffuses into the first block and the maturity can then increase to around 0.9 after 60 days. This gain in water for the first block is a loss for the second, which results in a lower than expected maturity near the interface. After 60 days the minimum maturity, near $x = 1$, is around 0.62. Near the outer surface, $x = 2$, we can again see the slight dip in maturity caused by the evaporation of water near the surface.

The corresponding moisture profiles are shown in Figures 12, 13. In particular in Figure 13 we can see that after 30 days there is little water anywhere in the block. The addition of the second block increases the moisture considerably. After 60 days there is still a significant amount of water left in the second block, so we expect the reaction to continue for some time.

The temperature profile is shown in Figure 14. The addition of the second layer insulates the first from the external energy and so we see the high temperature near $x = 1$ slowly diffuse through the block until after around 40 days the temperature is approximately constant for $x < 1$. The variation is then all in the second block. We see the usual peaks near $x = 1$

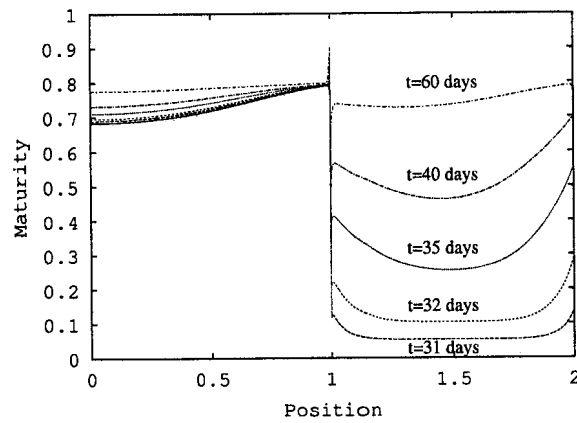


Figure 10: Evolution of the maturity profile during the second month of a two layer simulation

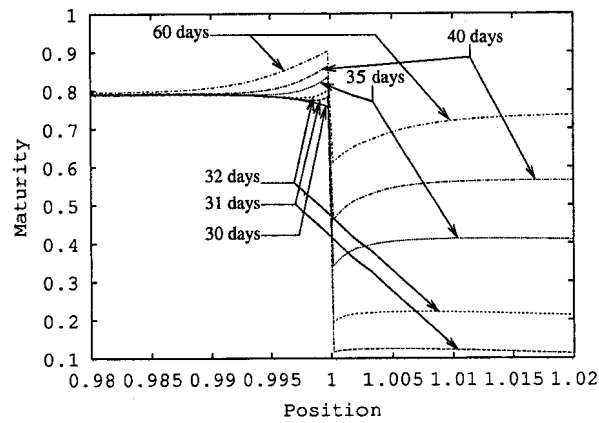


Figure 11: Evolution of the maturity profile around the interface

due to the high midday temperatures. The central part of the second block is originally cool but rapidly heats up since it is heated from both sides. At the end of the simulation the temperature profile shows no indication of the two stage building.

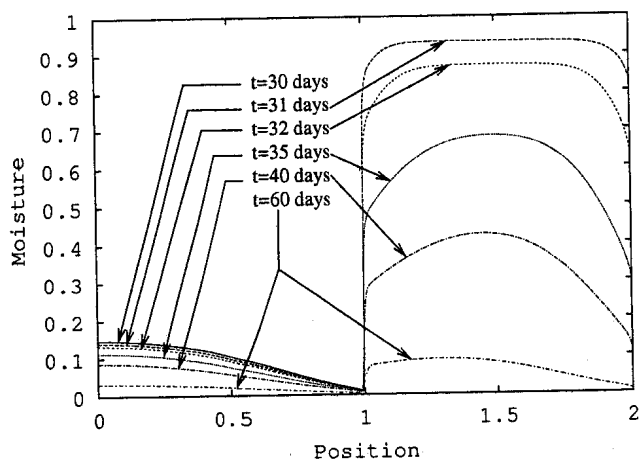


Figure 12: Evolution of the moisture profile during the second month of a two layer simulation

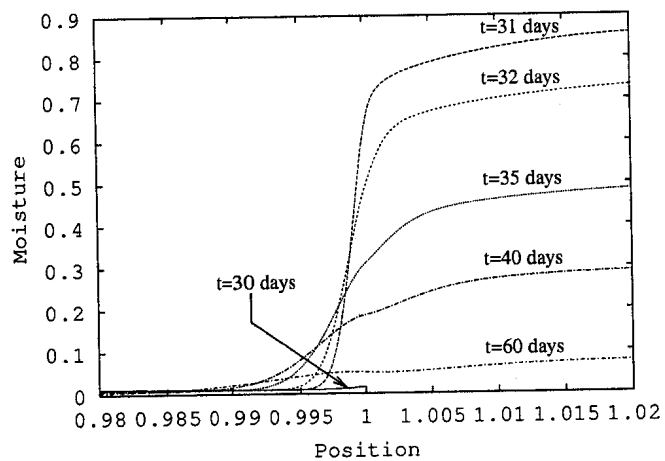


Figure 13: Evolution of the moisture profile around the interface

6 Conclusion

The main output of this work is the numerical scheme that can model the evolution of maturity, moisture and temperature of a concrete block through time. Results were presented for both short and long times.

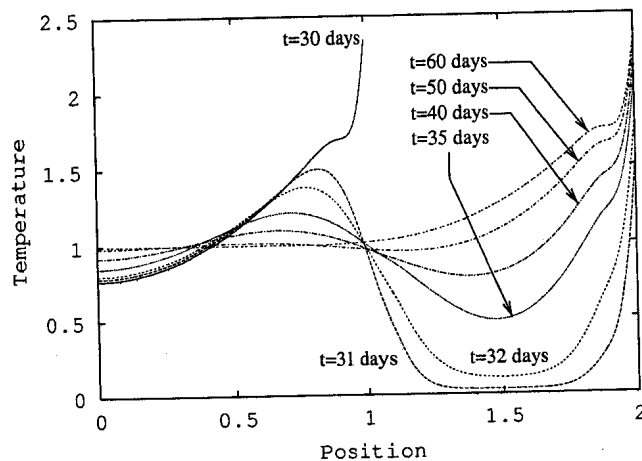


Figure 14: Evolution of the temperature profile during the second month of a two layer simulation

A number of interesting features were observed in the calculations. For short times, of the order of days, the maturity increases most rapidly near the free surface. However, over a long period this surface will be the least mature, due to the fact that water evaporates there and so is not available for the reaction. Of course over even longer time periods it is possible that water from the atmosphere could permit the reaction to slowly continue. When a second layer is added to the first then water can diffuse from the upper layer to the lower one. This results in the top of the lower layer becoming more mature than expected. The loss of water at the bottom of the upper layer leads to a decrease in maturity there. The bulk temperature slowly increased throughout the simulations, with only the top 20% reacting to the daily temperature fluctuations.

The analytical model showed good agreement with the numerical results for small times, but the neglect of the temperature variation in the maturity equation and the cooling condition at the free surface prevented it from being applicable over long times.

The graphs of moisture content showed that the free surface would always have a lower water content than deeper down in the block. In the two month simulations there was significantly more moisture away from the surface, at times around a factor 2. If the concrete surface is covered with an impermeable layer then when this extra water diffuses to the surface it could

easily bring the surface moisture above the specified limit for the applying the covering, leading to the damage described in [2].

The numerical and analytical temperature profiles highlighted perhaps the main drawback of the model, namely the boundary condition at $x = 0$. There we imposed no energy loss, which prevents any heat from leaving at this boundary. The results showed that this led to rather large temperature increases, particularly for the analytical model. In future work it will clearly be necessary to address this issue and presumably include some form of cooling condition, dependent upon the material below the initial block.

Acknowledgements

All contributors would like to thank Prof Yunus Ballim for introducing the problem and assisting in answering questions. T.G. Myers acknowledges support of this work under the National Research Foundation of South Africa grant number 2053289. J.P.F. Charpin acknowledges the support of the Claude Harris Foundation.

7 Nomenclature

c_c	Thermal capacity of concrete	880	$\text{J}\cdot\text{kg}^{-1}\cdot\text{K}^{-1}$
\bar{e}	Evaporation rate	1.8×10^{-9}	$\text{m}\cdot\text{s}^{-1}$
m	Maturity	0-1	ND
m_x	Parameter for the hydration heat release	0.15	ND
t	Time		s
τ	Time scale	1000	s
x	Cartesian coordinate		m
D_m	Moisture diffusivity in concrete	2×10^{-9}	$\text{m}^2\cdot\text{s}^{-1}$
E	Apparent activation energy of the reaction	35×10^3	J
H	Heat transfer coefficient	5	$\text{J}\cdot\text{K}^{-1}\cdot\text{m}^{-2}\cdot\text{s}^{-1}$
L	Length scale	3	m
Q_s	Heat received at the surface	-500	$\text{J}\cdot\text{m}^{-2}\cdot\text{s}^{-1}$
Q_x	Parameter for the hydration heat release	10^8	$\text{J}\cdot\text{m}^{-3}$
R	Gas constant	8.314	$\text{J}\cdot\text{K}^{-1}$
T	Non-dimensional temperature	0-1	ND
T_i	Initial temperature	295.5	K
ΔT	Typical temperature jump in the block	25	K
γ	Heat release coefficient due to hydration		$\text{J}\cdot\text{m}^{-3}$
η	Stoichiometric ratio for the hydration reaction	0.625	ND
θ	Moisture content	0-1	ND
θ_a	Ambient moisture content	0.05	ND
θ_i	Initial moisture content	1	ND
κ	Heat diffusion coefficient	1.37	$\text{J}\cdot\text{K}^{-1}\cdot\text{m}^{-1}\cdot\text{s}^{-1}$
μ	Reaction rate	1	s^{-1}
ρ_c	Density of concrete	2350	$\text{kg}\cdot\text{m}^{-3}$

References

- [1] Pavlik, J., Tydlitát, V., Cerný, R., Klečka, T., Bouska, P. and Rovnanikova, P. Application of a microwave impulse technique to the measurement of free water content in early hydration stages of cement paste. *Cement & Concrete Research* **33** (2003), 93-102.
- [2] West, R.P., Holmes, N. Predicting moisture movement during the drying of concrete floors using finite elements. *Construction & Building Materials* **19** (2005), 674-681.
- [3] Fowkes, N.D., Mambili Mamboundou, H., Makinde, O.D., Ballim, Y. and Patini, A. Maturity effects in concrete dams. *Proc. Mathematics in Industry Study Group South Africa 2004*, University of the Witwatersrand, (2004), 59-67.
- [4] Charpin, J.P.F., Myers, T.G., Fitt, A.D., Ballim, Y. and Patini, A. Modelling surface heat exchanges from a concrete block into the environment. *Proc. Mathematics in Industry Study Group South Africa 2004*, University of the Witwatersrand, (2004), 51-58.